Large-Scale Highly Ordered Chitosan-Core Au-Shell Nanopatterns with Plasmonic Tunability: A Top-Down Approach to Fabricate Core–Shell Nanostructures

By *Youn-Kyoung Baek, Seung Min Yoo, Taejoon Kang, Hwan-Jin Jeon, Kyounghwan Kim, Ji-Sun Lee, Sang Yup Lee, Bongsoo Kim,* and *Hee-Tae Jung**

A new strategy for fabricating highly ordered chitosan–Au core–shell nanopatterns with tunable surface plasmon resonance (SPR) properties is developed. This strategy combines fabrication of a chitosan nanopattern by using a soft-nanoimprint technique with selective deposition of Au nanoparticles onto the patterned chitosan surface. The SPR response can be tuned by controlling the features of the resulting Au shell/polymer hybrid pattern, which makes these materials potentially useful in ultrasensitive optical sensors for molecular detection.

1. Introduction

Plasmonic metal nanostructures are currently receiving much research interest due to their unique surface plasmon resonance (SPR) properties.[1–5] When the dimensions of such a nanostructure are smaller than the wavelength of the incident light, it exhibits an intense absorption band in a specific spectral region due to the collective oscillation of the conduction electrons. This absorption property allows such metal nanostructures to be employed in a variety of applications including biodetection, bioimaging, therapeutic treatment of cancer tissues, metal-enhanced fluorescence, surface-enhanced vibrational spectroscopies and solar screening.[6–13] Depending on the type of application, the desired SPR properties at a specific wavelength can be obtained by controlling the composition and features of the metal nanostructure.[14]

Several approaches to creating tunable plasmonic nanostructures have been developed, including the fabrication of dielectric-core metal-shell nanoparticles and anisotropic solid metal objects such as nanorods, nanocrystals, and nanotriangles.[15–20] Compared to other plasmonic nanoparticles, core–shell structures consisting of a dielectric core surrounded by a concentric metal thin layer have many advantages over other systems; in particular, they exhibit remarkable surface plasmon sensitivity due to the interaction between the plasmonic responses of the core and of a cavity.[21] Furthermore, their plasmonic absorption can be tuned precisely to the desired wavelength region by controlling the shape, size, and thickness of the dielectric core and the metallic shell.[22–25] In addition, new plasmonic features of the SPR resonance of the shell structures can be engineered by simply altering the core geometry so as to reduce symmetry.[16,17]

To date, most plasmon core–shell structures have been developed by the fabrication of individual metallo-dielectric nanostructures, even though a highly periodic core–shell nanostructure array is an ideal candidate for a wide range of applications requiring new plasmonic properties. Indeed, the integration of an individual plasmonic nanostructure into a one- or two-dimensional array gives rise to the strong coupling of surface plasmons in adjacent nanostructures, and leads to significant changes in the SPR absorption spectrum. For example, it has been reported that a Au nanoshell (AuNS) monolayer with a constant interparticle spacing can result in the enhancement of the absorption in the mid- or far-infrared spectral regions and that an individual AuNS can result in SPR properties across the visible and near-infrared (NIR) wavelength bands.[26] To achieve such goals, the dielectric-core metal-shell nanostructure needs to be highly periodic over a large area, and the fabrication method should be reproducible and reliable. Also, control over the dimensions of the features of the core–shell structure such as the interparticle spacing, size, and height has to be facile so that a wide range of surface plasmon properties can be generated. Unfortunately, however, most attempts recently made have focused on fabricating dielectric-core metal-shell particles, which resulted in somewhat irregular structures due to the difficulties in precisely controlling the geometry and in positioning the individual units at a desired location; these problems resulted in undefined SPR absorption.[12,27] Furthermore, the previous approaches to attaching metal nanoparticles to dielectric cores, which include the use of self-assembled monolayers (SAMs) and multistep processes to introduce functional groups,[15,28,29] require time-consuming sequential deposition steps. Despite of many recent efforts, creating patterned core–shell

[*] Y.-K. Baek, Dr. S. M. Yoo, H.-J. Jeon, K. Kim, J. S. Lee, Prof. S. Y. Lee, Prof. H.-T Jung
Department of Chemical and Biomolecular Eng. (BK-21)
Korea Advanced Institute of Science and Technology
Daejeon 305–701, Korea
E-mail: heetae@kaist.ac.kr
T. Kang, Prof. B. Kim
Department of Chemistry
Korea Advanced Institute of Science and Technology
Daejeon 305–701, Korea

DOI: 10.1002/adfm.201001051

plasmonic structures over a large area with well-defined SPR properties remains a key challenge.

In this study, we developed a new method for the fabrication of highly periodic arrays of dielectric-core metal-shell structures that generate well-defined absorption in the NIR wavelength region, which can be considered as a highly reliable top-down approach. A chitosan polymer containing abundant primary amine groups was employed as the dielectric core material, which means that various shell components can be attached. Large-area periodic chitosan patterns were fabricated by using combined soft and nanoimprint lithography, followed by selective deposition of metal shells onto the patterned chitosan surface, which generates an ordered core–shell patterned nanostructure. A proof-of-concept application of surface-enhanced Raman scattering (SERS) based detection of DNA hybridization on the chitosan–Au core–shell nanopatterns was also performed.

2. Results and Discussion

The overall strategy for fabricating large-area Au shell nanopatterns with a chitosan core template via combined soft and nanoimprint lithography followed by seed-mediated electroless Au plating is shown in **Figure 1**. It is important to emphasize that chitosan has significant advantages for the preparation of dielectric-metal core–shell nanostructures; the chitosan polymer has superior selectivity due to its abundant primary amine groups with respect to a wide range of metals and other functional components.[30] In fact, the silica and polystyrene nanoparticles that are commonly used as dielectric core particles require linker molecules such as SAMs or other multistep procedures to immobilize metal shells.[15,31] Thus, the amine functional groups of the chitosan polymer allow us to selectively immobilize a variety of biological components such as DNA, enzymes, and cells. Furthermore, the chitosan polymer has good physical and viscoelastic properties, as well as pH-responsive solubility for the fabrication of large-area nanopatterns with various features via soft lithography and aqueous solution processes at neutral and high pH.[32]

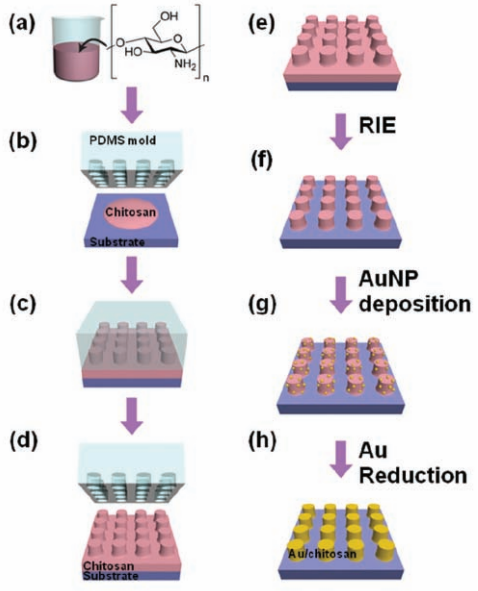

Figure 1. Schematic for the fabrication procedure of chitosan-core Au-shell nanopatterns. a) Fabrication of chitosan hydrogel. b) Location of chitosan droplet on the substrate. c) Pattern transfer using PDMS mold under constant pressure and temperature conditions. d) PDMS mold release from the patterned film. e) As-fabricated chitosan pattern. f) Removal of the residual layer by reactive ion etching (RIE). g) Deposition of Au nanoparticles. h) Au shell formation via electroless Au plating method.

Chitosan polymer was dissolved in a mixture of acetic acid and deionized water (18 MΩ cm) with a volume ratio of 1:2, and heated to 40°C (Figure 1a). After dropping a small volume of the chitosan solution onto the substrate, the patterned PDMS mold with the desired topographic features was placed on top of the chitosan polymer droplet (Figure 1b). The pattern was transferred to the underlying chitosan layer through suitable soft lithographic conditions with an applied pressure of 15–20 psi and a temperature of 90°C for ≈30 min (Figure 1c). The solvent of chitosan solution is evaporated and absorbed by PDMS mold during the hot embossing process, resulting in a solid gel consisting of entangled chitosan networks.[33] After removing the mold from the chitosan surface (Figure 1d), the chitosan pattern was successfully prepared over the entire substrate (Figure 1e). To isolate the chitosan pattern on the substrate, the residual chitosan layer on the substrate surface was removed by reactive ion etching (RIE) with a gas mixture of O_2 (10 sccm) and CF_4 (10 sccm) plasma at a chamber pressure of 12 mTorr and a power density of 50 W (Figure 1e). The resulting isolated chitosan pattern (Figure 1f) was then immersed in an aqueous solution of spherical Au nanoparticles (AuNPs) with an average diameter of 1.5 nm (Figure 1g). The AuNPs were prepared by the reduction of chloroauric acid with tetrakis(hydroxymethyl) phosphonium chloride (THPC).[34] The electroless plating of AuNPs onto chitosan was accomplished by reducing the aqueous Au plating solution in the presence of formaldehyde reductant for a given time (Figure 1h), which led to the formation of the patterned metal-shell chitosan-core structure. The resulting structure is referred to as a patterned chitosan–metal core–shell structure, although the bottom of the core is not covered by metal shells. The details of the reduction procedure are described in the Experimental Section.

Scanning electron microscopy (SEM) images of the as-fabricated chitosan pattern prepared with a PDMS stamp suggested that the well-ordered pattern with high fidelity was made on the substrate (**Figure 2**). The chitosan pattern was replicated by the PDMS stamp (see inset in Figure 2a) over a large area (7×7 mm^2), and consists of a hexagonally patterned array of cylindrical pillars with an average diameter (d) of 300 nm and an average height (h) of 300 nm (Figure 2a–c). This technique replicates a pattern from a master mold prefabricated on a solid substrate by conformal contact, so chitosan patterns with a wide range of feature shapes and dimensions can be prepared, provided that silicon masters with the desired features are used. In addition to the use of silicon masters with different features, the feature size and shape can be varied from a single prepattern by controlling the polymer film thickness and the reactive

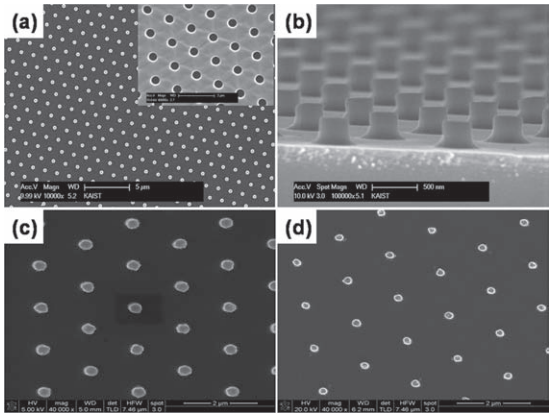

Figure 2. a–c) Representative SEM images of the replicated chitosan pattern with various magnifications (see the scale bars) and d) isolated chitosan pattern etched by carrying out O_2/CF_4 RIE for 21 s. The inset of (a) is a SEM image of PDMS mold used.

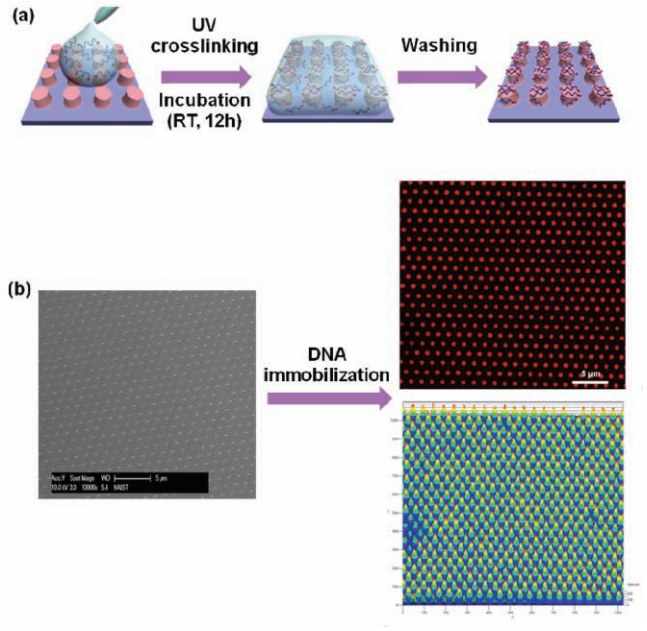

Figure 3. Immobilization of DNA on the chitosan pattern. a) Schematic of the fabrication of highly ordered DNA pattern based on the chitosan pattern. b) Representative SEM image of chitosan pattern etched for 21 s (left), a fluorescence image (upper right), and an intensity profile (lower right) of the isolated chitosan pattern after the immobilization of the Cy5-labeled DNA molecules. The fluorescence data were obtained using a confocal laser scanning microscope (Delta Vision RT, Applied Precision). The Cy5 florescence was excited at 640 nm and collected in the 685 nm optical window.

etching conditions.[34] RIE was performed to remove the residual chitosan layer that remained on the bottom, which is critical to the selective decoration of AuNPs onto the patterned chitosan surfaces (see Figure 1f,g). The SEM images of the chitosan patterns for various plasma etching times show that the residual layer was removed after plasma etching for 21 s, which results in the isolation of individual pillars (see Figure S1 in the Supporting Information). After plasma etching for 21 s (Figure 2d), however, the diameter of the isolated chitosan pillars was found to be also decreased from ≈300 nm in diameter before plasma etching to ≈100 nm (Figure 2c). This is because RIE not only removes the residual chitosan layer but also etches the chitosan pillars.

To validate the formation of a large-area, periodically isolated chitosan pattern having desirable characteristics, DNA molecules were immobilized onto the patterned chitosan surface. As shown in **Figure 3a**, Cy5-labeled 10 μM probe DNAs were spotted onto the chitosan pattern. The substrate was treated with UV cross-linking and then incubated at room temperature (RT) for 12 h for DNA immobilization. The binding method employing UV cross-linking[36] is expected to encourage the interaction of negative charges of DNA with the protonated amine groups of chitosan, resulting in the attachment of DNA to the chitosan surface. The fluorescence image and the corresponding intensity profile after the immobilization of the DNA molecules clearly showed well-isolated periodic fluorescence dots over a large area (Figure 3b), which confirms the selective immobilization of the DNA on the chitosan pattern. Furthermore, these results indicate that there are abundant amine groups on the patterned surface that are available for the binding of DNA, even though the chitosan undergoes etching under harsh conditions. Thus, the assembly strategy with chitosan patterns reported here makes it possible to fabricate optical sensing substrates and the nanopatterns of substrates for array-based detection of biomolecules.

To encapsulate Au shells on the patterned chitosan surface, AuNPs were deposited onto the chitosan pattern by soaking it in AuNP solution for 30 min. After subsequent rinsing and air drying, the AuNPs were reduced in a solution of formaldehyde with an aged mixture of chloroauric acid and potassium carbonate. A representative SEM image of the resulting Au shell/chitosan core pattern after Au reduction is shown in **Figure 4a**, together with the corresponding energy dispersive X-ray (EDX) spectra of a single core–shell (Figure 4b) and the substrate surface (Figure 4c). The chitosan pattern was etched for 21 s to prepare the isolated Au shell. As expected, the size of the resulting chitosan-core Au-shell pattern (Figure 4a) was considerably increased (d ≈ 375 nm) after Au reduction, compared to that of the chitosan pattern (d ≈ 200 nm), which indicates the formation of Au shells on the chitosan surface. The EDX results clearly verified the selective formation of an isolated Au shell pillar structure on the chitosan pattern. A high content (≈30 wt%) of Au was detected in the hybrid pillar nanostructure regions (Figure 4b), while there was no Au peak for the substrate surfaces (Figure 4c), which confirms the selective deposition of the AuNPs on the isolated chitosan pillars.

The SPR properties of the resulting highly ordered chitosan–Au core–shell nanopatterns are expected to be tunable depending on their geometrical conditions. The features of Au shell nanopatterns are strongly influenced by the geometrical conditions of the chitosan cores, which can be dramatically changed by simply controlling the RIE time (Figure S1, Supporting Information). **Figure 5** shows the changes in UV-vis/NIR absorption spectra of the resulting Au patterns according to etching time increment of the chitosan cores. The SPR absorption

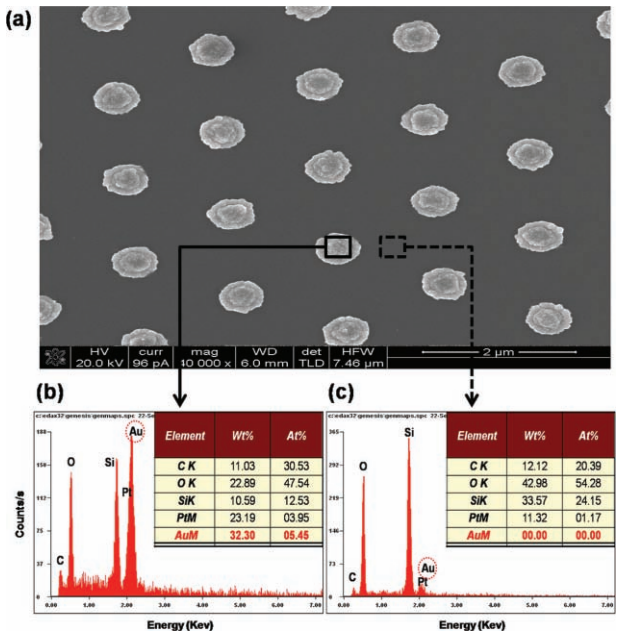

Figure 4. a) SEM images of Au shell nanopattern incorporated with chitosan pattern etched by carrying out O_2/CF_4 RIE for 21 s. b–c) EDX analysis of (a). The characterization was carried on a Phoenix EDAX system (GENESIS 4000) attached to the SEM at the acceleration voltage of 10 keV. The signals were collected in the two rectangular areas in (a): Au shell pattern and SiO_2 substrate. The results shown in (b) and (c) are obained from Au shell pattern and bottom substrate, respectively. The insets of (b) and (c) are element contents collected from the respective selected area. Pt element detected in data is due to the coating procedure for SEM observation.

measurements were carried out at RT on the patterned nanostructures with unpolarized light at normal incidence. Reduction of AuNPs was carried out for 45 min. There are no specific peaks in the wavelength region for the as-synthesized AuNP solution (mean diameter = 1.5 nm) and the as-fabricated chitosan pattern (see Figure S2, Supporting Information). However, the spectrum of the resulting Au pattern combined with the non-etched chitosan pattern (0 s, blue line) contains a broad plasmon peak (average absorption maximum, $\lambda_{max} \approx 686$ nm), which is generally observed for aggregated AuNPs.[8] After 3 s of RIE (pink line), the SPR absorption band rises slightly in the long wavelength region, as has been observed in previous spectroscopic studies of Au platelet solutions.[15,37] When the RIE time was increased to 9 s (green line), a broad plasmon peak appeared at a longer wavelength, which indicates the formation of a uniform Au shell layer on each chitosan pillar. A further increase in the RIE time (12 s, orange line) resulted in a blue-shift in the plasmon peak and in a significant increase in its intensity, with maximum absorption at 1812 nm, which is due to Au shell thickening.[15] After 21 s of RIE (red line), a narrow sharply defined absorption peak (1780 nm) in the NIR wavelength region was observed, which confirms the presence of a well-isolated chitosan-core Au-shell pattern and is due to localized surface plasmon resonance (LSPR) coupling from the isolated Au shell dot array. It is noteworthy that our approach for fabricating core–shell nanopatterns is considerably reproducible. As shown in Figure S3 in the Supporting Information, the absorption spectra taken from the five different positions on a single pattern and five different replicates fabricated with the chitosan cores etched for 21 s show the slight wavelength fluctuation with a $\lambda_{max} \approx 1780$ nm.

This behavior is probably due to the number of AuNPs deposited on the chitosan surface, as shown in **Figure 6**. The number of Au adsorbates decreases as the RIE time increases because the surface area of the chitosan decreases with the increase of etching time. Thus, the changes in the number of Au nuclei result in different growth of the deposited AuNPs, which causes the changes in the SPR response. The maximum absorption peak in the visible wavelength region obtained from the pattern without RIE suggests that the AuNPs aggregate on the patterned chitosan surfaces (Figure 6a). When the chitosan pattern is isolated by the removal of the residual layer, a relatively small number of AuNPs could easily coalesce further into Au platelets, which leads to the formation of a continuous Au shell and shell thickening on the isolated chitosan surface under the same Au reduction time conditions (Figure 6b). Thus, the strategy reported in this paper enables the fabrication of Au shell nanopatterns with a defined resonance absorption and SPR tunability from the visible to NIR wavelength regions.

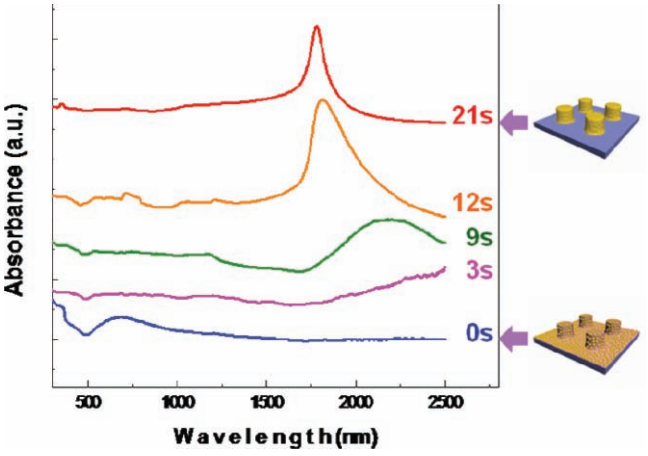

Figure 5. UV–vis/NIR absorption spectra of Au shell patterns incorporated with chitosan cores etched under various time conditions: 0, 3, 9, 12, and 21 s. The extinction maxima are 686 nm (0 s), 2204 nm (9 s), 1812 nm (12 s), and 1780 nm (21 s).

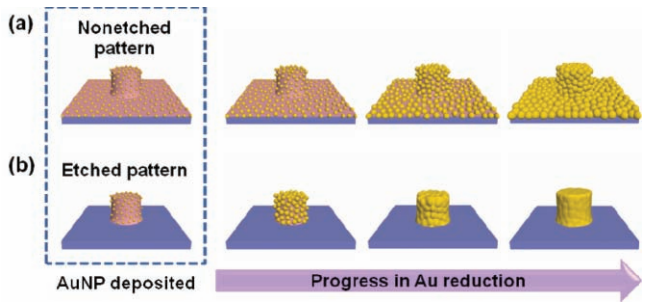

Figure 6. Illustration for Au reduction process of AuNPs deposited on a) as-fabricated chitosan pattern and b) isolated chitosan pattern treated by plasma etching.

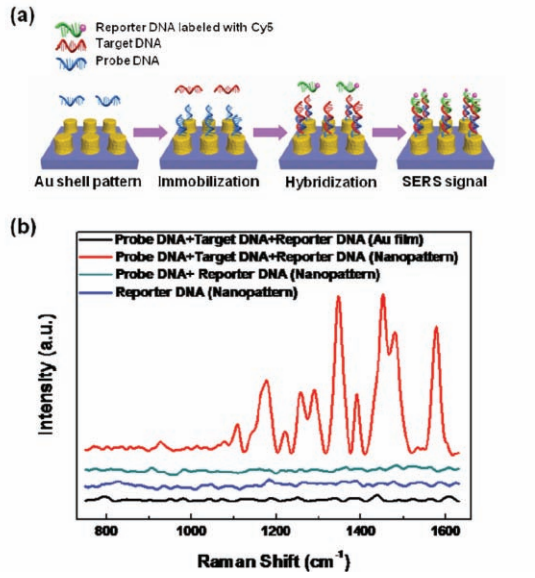

Figure 7. SERS detection of DNA hybridization on the chitosan-core Au-shell nanopattern. a) Schematic representation for the detection of target DNAs on the chitosan-core Au-shell nanopattern. b) SERS spectra of chitosan-core Au-shell nanopattern system (red spectrum), and that of Au film (black spectrum) prepared with probe-complementary target-reporter DNAs. Control experiments were carried out with only reporter DNAs (blue spectrum) and with probe DNAs and reporter DNAs (green spectrum) on the Au shell nanopatterns. All SERS experiments were carried out using a micro-Raman system and the samples were excited by 300 μW of a 633 nm He–Ne laser.

To demonstrate the proof-of-concept biosensing applications of the chitosan–Au core–shell nanopatterns, SERS based detection of DNA hybridization was performed. The 10 μM probe DNAs were spotted and incubated onto both Au shell nanopatterns and Au film substrate (**Figure 7a**). The 5 μM target DNAs, which are complementary to probe DNAs and Cy5-labeled reporter DNA, were directly hybridized with Au shell nanopatterns. The resultant substrates were incubated with Cy5-attached reporter DNA and SERS spectra from two different substrates were measured in ambient conditions. As shown in Figure 7b, the resulting chitosan–Au core–shell nanopattern (red spectrum) provided strong SERS spectra of Cy5 while the resulting Au film (black spectrum) substrate exhibited a very low signal. To check cross reactivity and nonspecific adsorption, control experiments of the reporter DNAs (blue spectrum), probe DNAs and reporter DNAs (green spectrum) on the Au shell nanopatterns, were carried out, resulting in no discernible SERS signals. Thus, the Au shell system exhibits SERS activity for the detection of DNA hybridization. Therefore, the chitosan–Au core–shell nanopatterns developed in this study can be employed in various biosensing applications as such as the detection of pathogenic microorganisms and single nucleotide polymorphisms, biomarker research, and disease diagnosis.

3. Conclusion

In summary, we have prepared highly ordered chitosan–Au core–shell nanopatterns by using a chitosan core template via combined soft and nanoimprint lithography followed by seed-mediated electroless Au plating. The Au shell-chitosan core patterned structures generated in this way have several notable features. First, highly ordered Au shell structures with various features can be readily integrated over a large area by employing patterned chitosan matrices via a reliable top-down approach. Second, the surface plasmon absorption of the resulting patterned substrate can be precisely tuned by simply controlling the geometry of the PDMS stamp and the fabrication conditions. Third, the resulting core–shell array exhibits well-defined and narrow absorption in the NIR wavelength region. This large-area chitosan pattern of a well-ordered plasmonic structure exhibiting SPR tunability can be employed in many practical applications including optical, photonic, chemical, and biosensing devices; one proof-of-concept application of the system to highly sensitive SERS-based detection of DNA molecules was demonstrated. Thus, the strategy for making chitosan-core Au-shell nanopatterns reported in this paper should be generally useful for the fabrication of optical sensing substrates based on SPR tunability. Further studies are in progress to investigate the effects of the feature dimensions on the surface plasmon properties.

4. Experimental Section

Preparation of Chitosan Nanopattern: We used a silicon master consisting of a hexagonally patterned array of cylindrical posts, each 400 nm in diameter and 800 nm in height. The whole area of the pattern was 7 × 7 mm^2. The PDMS mold was fabricated by pouring the mixture of PDMS prepolymer (Sylgard 184 A:B–10:1, Dow Corning) onto the silicon master and curing at 60°C for 12 h. Chitosan polymer (Aldrich, ≈50 to 190 kDa) was dissolved in a mixture of acetic acid (Sigma–Aldrich) and deionized water (18 MΩ cm) with a volume ratio of 1:2, and heated to 40°C. The viscosity of the chitosan solution was controlled by modulating the chitosan polymer concentration. The substrates (Si wafer or quartz glass) were cleaned with O_2 plasma (100 sccm) for 5 min at a pressure of 32 mTorr and a power of 100 W. A small volume of the chitosan solution was dropped onto the substrate, and the patterned PDMS mold was placed on top of the chitosan polymer droplet. A slight pressure (≈15 to 20 psi) was applied onto top of the PDMS mold with a small weight to ensure a good conformal contact. After heating at 90 °C for ≈30 min and then cooling to RT, the PDMS mold was carefully taken off from the substrate. The residual chitosan layer that remained on the bottom of the imprinted structure was subsequently removed by carrying out O_2/CF_4 RIE operated at a flow of 10/10 sccm, a chamber pressure of 12 mTorr and an RF power of 50 W.

Preparation of the Au Nanoparticle Solution: 1.5 mL of aqueous solution of sodium hydroxide (0.2 M, Aldrich) was mixed with 45.5 mL of deionized water with vigorous stirring, followed by the addition of 1 mL of an aqueous solution of the reducing agent THPC solution (Aldrich, 1.2 mL of 80% aqueous solution diluted to 100 mL with water). Afterwards, within 2 min, 2 mL of the metal salt chloroauric acid (25 mM, Sigma–Aldrich) was quickly added to the mixture, resulting in formation of orange-brown solution. The Au nanoparticle solution was stored at 4 °C until use.

Electroless Au Plating Process: Aqueous Au plating solution was produced by the addition of 3 mL of 5 mM chloroauric acid solution to 200 mL of 1.8 mM aqueous potassium carbonate (Sigma–Aldrich). The solution was then stored for a minimum of 24 h. Under continuous stirring, Au nanoparticle-attached chitosan substrates were vertically introduced to 12 mL of the aged Au plating solution, followed by adding 0.5 mL of 2 vol% formaldehyde solution (Sigma). After a 45 min with vigorous stirring, the substrates were rinsed with deionized water and air-dried.

Absorption Measurement: The optical absorbance of the patterns was measured using a V-570 UV/VIS/NIR spectrophotometer (JASCO). During measurement, the Au nanopatterned quartz substrate was maintained in an upright position in a thin film sample holder. Unpolarized white light from a tungsten halogen lamp was focused on the sample, with a spot size of 7 mm.

Immobilization of DNA on the Chitosan Nanopattern: Cy5-labeled 10 μM probe DNA (5'Cy5-TGGCTGCTTCTAAGCCAACATCCT-3', GenoTech Co. Daejeon, Korea) in 3× SSC (0.45 M NaCl, 15 mM $C_6H_5Na_3O_7$, pH 7.0) solution were spotted onto the chitosan pattern. The substrate was treated with UV cross-linking and then incubated at RT for 12 h for DNA immobilization. To remove the unbound probe DNA, the substrate was washed with 2× SSC buffer containing 0.2% (w/v) SDS for 5 min.

Hybiridization of DNA on Chitosan–Au Core–Shell Nanopatterns for SERS Detection: After treated with 1 M dithiothreitol (DTT; Sigma–Aldrich) and purified using NAP-5 column (GE healthcare, UK), 10 μM probe DNAs (5'SH-CATGGCCTTCACTGGCTGT-3') in 1 M KH_2PO_4 (pH 6.75) were spotted onto both Au shell nanopatterns and Au film substrate at RT for 24 h. To remove the unbound probe DNAs, the substrates were washed with 0.2% (w/v) SDS for 5 min. The 5 μM of target DNAs (5'-CTACGACGGTATCTGATACAGCCAGTGAAGGCCATG-3'), which are complementary to probe DNAs and Cy5-labeled reporter DNA, were directly added to the hybridization solution containing 6× SSPE (0.9 M NaCl, 10 mM $NaH_2PO_4{\cdot}H_2O$, 1 mM EDTA, pH 7.4), 20% (v/v) formamide (Sigma-Aldrich), and 0.1% (w/v) SDS and hybridized with Au shell nanopatterns at 30°C for 6 h. After washing with 2× SSPE buffer containing 0.1% (w/v) SDS for 5 min, the resultant substrates were incubated with Cy5-attached reporter DNA (5'-ATCAGATACCGTCGTAG-3') in PBS containing 0.1% (w/v) SDS at 30°C for 2 h. After washing with PBS containing 0.1% (w/v) SDS for 5 min, rinsing twice with deionized water, and drying under nitrogen stream, SERS spectra from two different substrates were measured in ambient conditions.

Supporting Information

Supporting Information is available from the Wiley Online Library or from the author.

Acknowledgements

This work was supported by the World Class Universities project (R32-2008-000-10142-0) and the National Research Laboratory Program (R0A-2007-000-20037-0) from the Ministry of Education, Science and Technology (MEST) through the National Research Foundation (NRF). The work of S.Y.L. was also supported by the Conversing Research Center Program of MEST through the NRF (2009-0082332).

Received: May 24, 2010
Revised: July 15, 2010
Published online: September 14, 2010

[1] M. E. Stewart, C. R. Anderton, L. B. Thompson, J. Maria, S. K. Gray, J. A. Rogers, R. G. Nuzzo, *Chem. Rev.* **2008**, *108*, 494–521.
[2] M. Hu, J Chen, Z.-Y. Li, L. Au, G. V. Hartland, X. Li, M. Marquez, Y. Xia, *Chem. Soc. Rev.* **2006**, *35*, 1084–1094.
[3] A. J. Haes, R. P. Van Duyne, *J. Am. Chem. Soc.* **2002**, *124*, 10596–10604.
[4] W. Wei, S. Li, J. E. Millstone, M. J. Banholzer, X. Chen, X. Xu, G. C. Schatz, C. A. Mirkin, *Angew. Chem. Int. Ed.* **2009**, *48*, 4210–4212.
[5] J. N. Anker, W. P. Hall, O. Lyandres, N. C. Shah, J. Zhao, R. P. Van Duyne, *Nat. Mater.* **2008**, *7*, 442–453.
[6] X. Huang, I. H. El-Sayed, W. Qian, M. A. El-Sayed, *J. Am. Chem. Soc.* **2006**, *128*, 2115–2120.
[7] L. R. Hirsch, R. J. Stafford, J. A. Bankson, S. R. Sershen, B. Rivera, R. E. Price, J. D. Hazle, N. J. Halas, J. L. West, *Proc. Natl. Acad. Sci. USA* **2003**, *100*, 13549–13554.
[8] Y. Wanga, W. Qian, Y. Tan, S. Ding, *Biosens. Bioelectron.* **2008**, *23*, 1166–1170.
[9] F. Tam, G. P. Goodrich, B. R. Johnson, N. J. Halas, *Nano Lett.* **2007**, *7*, 496–501.
[10] R. Bardhan, N. K. Grady, J. R. Cole, A. Joshi, N. J. Halas, *ACS Nano* **2009**. *3*, 744–752.
[11] H. Wang, J. Kundu, N. J. Halas, *Angew. Chem. Int. Ed.* **2007**, *46*, 9040–9044.
[12] S. S. Shankar, A. Rai, A. Ahmad, M. Sastry, *Chem. Mater.* **2005**, *17*, 566–572.
[13] E. Hutter, J. Fendler, *Adv. Mater.* **2004**, *16*, 1685–1706.
[14] C. Loo, A. Lin, L. Hirsch, M. H. Lee, J. Barton, N. J. Halas, J. West, R. Drezek, *Technol. Cancer Res. Treat.* **2004**, *3*, 33–40.
[15] S. J. Oldenburg, R. D. Averitt, S. L. Westcott, N. J. Halas, *Chem. Phys. Lett.* **1998**, *288*, 243–247.
[16] H. Wang, D. W. Brandl, F. Le, P. Nordlander, N. J. Halas, *Nano Lett.* **2006**, *6*, 827–832.
[17] H. Wang, Y. Wu, B. Lassiter, C. W. Nehl, J. H. Hafner, P. Nordlander, N. J. Halas, *Proc. Natl. Acad. Sci. USA* **2006**, *103*, 10856–10860.
[18] A. M. Funston, C. Novo, T. J. Davis, P. Mulvaney, *Nano Lett.* **2009**, *9*, 1651–1658.
[19] A. Tao, P. Sinsermsuksakul, P. Yang*Nat. Nanotechnol.* **2007**, *2*, 435–440.
[20] S. S. Shankar, A. Rai, B. Ankamwar, A. Singh, A. Ahmad, S. Sastry, *Nat. Mater.* **2004**, *3*, 482–488.
[21] M. W. Knight, N. J. Halas, *New J. Phys.* **2008**, *10*, 105006.
[22] G. Kaltenpoth, M. Himmelhaus, L. Slansky, F. Caruso, M. Grunze, *Adv. Mater.* **2003**, *15*, 1113–1118.
[23] J. B. Jackson, N. J. Halas, *J. Phys. Chem. B* **2001**, *105*, 2743–2746.
[24] H. Wang, F. Tam, N. K. Grady, N. J. Halas, *J. Phys. Chem. B*, **2005**, *109*, 18218–18222.
[25] S. J. Oldenburg, J. B. Jackson, S. L. Westcott, N. J. Halas, *Appl. Phys. Lett.* **1999**, *75*, 2897–2899.
[26] S. Lal, N. K. Grady, J. Kundu, C. S. Levin, J. B. Lassiterde, N. J. Halas, *Chem. Soc. Rev.* **2008**, *37*, 898–911.
[27] R. Bardhan, R. Neumann, N. Mirin, H. Wang, N. J. Halas, *ACS Nano* **2008**, *3*, 266–272.
[28] N. L. Lala, T. C. Deivaraj, J. Y. Lee, *Colloids and Surf., A* **2005**, *269*, 119–124.
[29] T. Ji, V. G. Lirtsman, Y. Avny, D. Davidov, *Adv. Mater.* **2001**, *13*, 1253–1256.
[30] M. J. Laudenslager, J. D. Schiffman, C. L. Schauer, *Biomacromolecules* **2008**, *9*, 2682–2685.
[31] W. Shi, Y. Sahoo, M. T. Swihart, P. N. Prasad, *Langmuir* **2005**, *21*, 1610–1617.
[32] H. Yi, L. Wu, W. E. Bentley, R. Ghodssi, G. W. Rubloff, J. N. Culver, G. F. Payne, *Biomacromolecules* **2005**, *6*, 2881–2894.
[33] I. Park, J. Cheng and A. P. Pisano, *Appl. Phys. Lett.*, **2007**, *90*, 093902.
[34] D. G. Duff, A. Baiker, P. P. Edwards, *Langmuir* **1993**, *9*, 2301–2309.
[35] J. M. Jung, F. Stellacci, H.-T. Jung, *Adv. Mater.* **2007**, *19*, 4392–4398.
[36] G. C. Vivian, M. Michael, A. Francisco, M. Aldo, K. Raju, C. Geoffrey, *Nat. Genet.* (Suppl.) **1999**, *21*, 15–19.
[37] J. Wiesner, A. Wokaun, *Chem. Phys. Lett.* **1989**, *157*, 569–575.